



On the seismic response of shallow-buried rectangular structures



E. Debiasi, A. Gajo*, D. Zonta

Dipartimento di Ingegneria Civile, Ambientale e Meccanica, Università di Trento, Via Mesiano 77, I-38123 Povo, Trento, Italy

ARTICLE INFO

Article history:

Received 21 April 2011

Received in revised form 28 February 2013

Accepted 30 April 2013

Available online 19 June 2013

Keywords:

Seismic response

Soil–structure interaction

Underground structures

Cut-and-cover

Frictional interface

ABSTRACT

Compared to bridges, underground structures are inappropriately regarded as less crucial components of road infrastructure in view of their supposedly low seismic vulnerability. The literature indicates, however, that shallow-buried rectangular structures, such as box culverts or rectangular tunnels, can be affected by shaking failure. To avoid the complexity of a fully non-linear soil–structure interaction analysis, a number of simplified methods have been proposed in recent years, which have gained popularity among designers. The aim of this paper is to investigate the applicability limits of such simplified analyses. The study compares the results obtained using simplified approaches with those emerging from non-linear static soil–structure interaction analyses, accounting for the following effects: the frictional behavior of the soil–structure interface, the geometry of the box structure, the overburden depth, the maximum PGA, and the increasing soil stiffness with increasing depth. The outcomes of the analysis indicate that shallow-buried rectangular structures are strongly affected by non-linear frictional effects at the soil–structure interface. The soil–structure interaction under seismic condition is shown to change smoothly from the condition of deep burial to the condition of “null overburden depth”. For a given aspect ratio, stiff, shallow-buried rectangular structures prove to be affected more deeply by sliding at the soil–structure interface than flexible structures and, for low aspect ratios, these structures may undergo a rigid rotation (rocking) that may even involve a partialization of the base foundation. For a reliable evaluation of member forces from racking distortions, rocking must be carefully taken into account.

© 2013 Elsevier Ltd. All rights reserved.

1. Introduction

There is no doubting that underground structures play an important part in the infrastructure of modern society, since they are involved in a number of applications ranging from storage to transportation systems. In seismic areas, the support for underground facilities must be designed for static overburden loads and for the additional forces due to soil–structure interaction under seismic conditions.

It is generally assumed that underground structures suffer appreciably less damage under seismic conditions than structures on the surface and, in particular, that such damage diminishes with increasing overburden depth (Hashash et al., 2001). Underground facilities built in soils are expected to suffer more damage than those constructed in rock. Special attention must be paid to cut-and-cover structures, i.e. those built in an open excavation where the backfill is subsequently placed over the finished structure. Such structures typically have a rectangular cross-section (*box-type* or *rectangular* tunnels) and are generally larger than circular tunnels, and they lie at shallow depths, usually in soils, the backfill often

having different properties from the surrounding soil. These conditions make the effects of soil–structure interaction particularly important. Box-type tunnels are also frequently built in urban areas (often adjacent to structures above ground that may be involved in the collapse of tunnels) and they are generally of strategic importance in highway and railway transportation systems.

Box-type tunnels are designed to withstand ground failure and ground shaking (Bobet et al., 2008). Ground failure includes shear displacements due to active faults intersecting the tunnel, soil liquefaction, slope instability, tectonic uplift and subsidence. Ground shaking is due to propagating waves distorting the support, i.e. compression/extension along the longitudinal axis, longitudinal bending and racking. Judging from the literature, racking distortion is considered the most critical and is induced mainly by vertically propagating shear waves (Merrit et al., 1985).

Like ovaling deformation of circular tunnels, racking distortions of rectangular tunnels can be analyzed with different degrees of refinement, using *simplified* linear, pseudo-static models (in which the inertial terms are neglected) or *complex*, fully non-linear, dynamic soil–structure interaction analyses. Simplified pseudo-static analyses may or may not take soil–structure interaction into account. Neglecting soil–structure interaction means that the structure is assumed to follow the free-field deformation of the ground (*free field approach*, Hendron and Fernández, 1983; Merrit

* Corresponding author. Tel.: +39 0461 882519; fax: +39 0461 882599.

E-mail address: alessandro.gajo@ing.unitn.it (A. Gajo).

URL: <http://www.ing.unitn.it/~gajoal/> (A. Gajo).

et al., 1985). This simplification may lead to unsafe results, however, especially when the structure is more flexible than the surrounding soil (Huo et al., 2006), and that is why several analytical and numerical methods have been proposed to take soil–structure interaction into account in *simplified* linear approaches. Most of these methods address circular tunnels (Hendron and Fernández, 1983; Merrit et al., 1985), while a few have focused on rectangular tunnels (Wang, 1993; Penzien and Wu, 1998; Penzien, 2000; Huo et al., 2006). Common assumptions of these *simplified* analyses are: plane strain conditions; linear-elastic deformations of ground and structure; and, with the exception of Wang (1993), pseudo-static conditions. The *simplified* analytical relationships (Penzien, 2000; Huo et al., 2006) also assume a great overburden depth and no-slip (i.e. *tied*) conditions at the soil–structure interface, with further simplifying assumptions typical of each method.

Simplified analyses usually neglect important aspects of soil–structure interaction, such as soil-stiffness degradation with increasing cyclic strain amplitude, and the role of friction at the soil–structure interface. Based on the analytical solution provided by Huo et al. (2006) and Bobet et al. (2008) recently suggested a practical iterative method for accounting, within the *simplified* approach, for soil stiffness degradation with increasing amplitudes of cyclic loading. These authors were possibly the first to consider the effects of friction at the soil–structure interface of buried rectangular structures, by comparing *simplified* analyses with the non-linear, dynamic numerical analyses performed by Huo (2005), who used a non-linear elastic constitutive model based on the extended Masing rules (Masing, 1926). Huo et al. (2005) showed that a portion of soil around the buried structure undergoes smaller strains than the surrounding soil, and consequently suffers less stiffness degradation. The size of this portion of soil increases with the friction at the soil–structure interface. Non-linear soil behavior leads to larger structural deformations than linear soil behavior; in particular, ‘a tied interface decreases structure deformations about 5–10% with respect to a frictional interface’. Unfortunately, these considerations were not associated with a range of validity in terms of the rectangular structure’s flexibility. Bobet et al. (2008) emphasized that this 5–10% underestimation of the deformations stemming from the assumption of a tied interface partially compensates for the overestimation of the structural deformation (15–20%) deriving from the assumption of a great overburden depth. The method proposed by Bobet et al. (2008) hinges on the assumption that the buried structure is stiffer than the surrounding soil, so it is not suitable for modeling structures undergoing significant damage. This suggests that the general conclusion reached by Huo et al. (2005) (i.e. that the soil portion around the buried structure suffers less stiffness degradation than the surrounding soil) only holds true for stiff structures, whereas for flexible structures we can expect the surrounding soil to suffer the greatest stiffness degradation.

More recently, Bobet (2010) published the results of an analysis conducted on circular and 4-sided rectangular tunnels either perfectly tied or with null friction at the soil–structure interface, but always assuming a great buried depth and perfectly elastic soil.

The earlier *simplified* analyses performed by Bobet et al. (2008) were the first attempt to account for the effects of shallow depths, friction at the soil–structure interface, and the geometry of 4-sided rectangular structures, but they did not exhaustively investigate the whole possible range of the flexibility ratio (which is the ratio of the racking stiffness of the surrounding ground to that of the structure). The effect of depth was analyzed for a perfectly tied interface, while the role of friction at the soil–structure interface was only analyzed for very deeply-buried structures. A number of issues thus remain unclear for shallow-buried, 4-sided rectangular structures, particularly concerning the interrelated effects of

shallow depths, friction at the soil–structure interface, the geometry of the rectangular structure and the maximum peak acceleration, over a wide range of flexibility ratios. The effects of increasing soil stiffnesses at greater depths has likewise never been addressed; nor has the behavior of 3-sided rectangular structures (involving two shallow footings instead of a bottom slab), except for a few comments from Anderson et al. (2008), who failed to mention how they took the rotational stiffness of the shallow footings into account in evaluating the flexibility ratio of the buried structure.

Although *simplified* analyses have been incorporating higher and higher levels of complexity in most recent works, and consequently seem to be losing their initial *simplicity*, they generally remain *simplified* in that they neglect important aspects of non-linear soil response and they are not restricted to a particular case study, trying instead to draw general conclusions, using elementary soil models without considering soil layering and geometrical details. Despite their limitations, such *simplified* analyses remain very important for design purposes because they enable the most important variables governing seismic response to be identified, thereby facilitating pre-dimensioning, so they are a preliminary step in any refined non-linear dynamic analysis. Simplified methods are also the basis of fragility models commonly adopted in vulnerability analyses (Basöz and Mander, 1999; HAZUS-MH MR3, 2003, for shallow-buried structures, see also Debiasi et al., 2012).

Acknowledging the importance of *simplified* analyses, this work aims to expand the scope of these methods by exploring the non-linear effects due to friction at the soil–structure interface, which have not been considered in the analyses published to date. In particular, our aim is to highlight the joint effects of non-linear behavior at the frictional soil–structure interface, small overburden depths and large ground peak accelerations, over a wide range of structure to soil stiffness ratios. Both 3-sided and 4-sided shallow-buried rectangular structures are considered. Thus, in the remainder of this paper we analyze the seismic behavior of buried rectangular structures over a wide range of flexibility ratios, accounting for the effect of the following variables:

- the type of soil–structure interface (either perfectly tied or frictional) on deep- and shallow-buried structures;
- the geometry of the cross-section (in terms of the aspect ratio, i.e. the width to height ratio, L/H);
- the overburden depth (in the range of low ratios of overburden depth to structure width typical of such shallow-buried structures).

In addition, the effects of maximum peak ground acceleration and the non-homogeneous soil stiffness (where soil stiffness increases with depth) have been taken into account.

The results were obtained using either pseudo-static or dynamic finite element modeling (FEM) with ABAQUS (Hibbitt et al., 2009), assuming a linear behavior for both the soil and the structure, and a perfectly tied or frictional soil–structure interface.

The main finding emerging from the numerical analyses is that shallow-buried rectangular structures are more affected by non-linearities (at the soil–structure interface) and by the initial stress conditions (which are influenced by the construction method). This is fairly reasonable due to the small confining pressure and the assumed frictional behavior of the soil and the soil–structure interface. The soil–structure interaction under seismic conditions is shown to change smoothly from the condition of deep burial to the condition of “null overburden depth”. An order of magnitude is given for the minimum depth above which the dynamic soil–structure response is typical of very deep structures. For a given aspect ratio, stiff, shallow-buried rectangular structures prove to be more affected by sliding at the soil–structure interface than

flexible structures. For low aspect ratios, moreover, stiff structures may be affected by a rigid rotation (rocking) that may even induce a partialization of the base foundation. Although never shown before, a rigid rotation of the underground structure may occur even in deeply-buried structures with a tied soil–structure interface, though it is in shallow-buried structures with a frictional soil–structure interface that rocking is most severe. For a reliable evaluation of the member forces from racking distortions, rocking must be carefully taken into account.

The rest of the paper is organized as follows. Section 2 provides details of the finite element model and the underlying assumptions used for the pseudo-dynamic analyses. Section 3 contains some preliminary observations that enable us to restrict the complexity of the problem. In particular: we highlight the effect of non-linearity, rocking, foundation partialization and soil detachment in the response of shallow-buried box sections; we define the critical burial depth below which the soil interface can be assumed to be tied. At this point, we conclude that the interface's behavior is virtually tied below the critical depth D_{Co} , so there is no need to refine the model. Above said critical depth, the response is sensitive to the interface conditions, and it departs all the more from the ideal tied condition the shallower the burying depth and the higher the peak acceleration. Since we found that the behavior of a shallow-buried structure changes gradually from the deep-buried condition to the null overburden condition, in Section 4 we concentrate our analysis on the latter limit case. More specifically, we analyze the effect of the flexibility ratio, structural geometry, peak ground acceleration and Poisson's ratio. Some concluding remarks and recommendations in view of the usage of these results in practical design are provided at the end of the paper.

To connect the results of this study to the existing literature, we have chosen to present the results in much the same way as in Wang (1993), i.e. in the form of practical design charts plotting the relative racking stiffness (the ratio of structural distortion to free-field racking displacements) versus the flexibility ratio. Since the structural member forces are not obviously affected by rigid body motions, however, we emphasize the need to account for the rigid rotation in order to calculate the racking distortions correctly.

2. Background assumptions of the analysis

In this section we state the background assumptions of the parametric analysis presented later on, i.e. the types of structure investigated, the input parameters considered, the finite element model used, and the output format of the analyses.

2.1. Types of structure and geometrical parameters

The types of structure investigated are the 3-sided and 4-sided rectangular frames, depicted in Fig. 1, of width L , height H and overburden depth D_0 , founded at a level D_B above the bedrock. In the case of 3-sided frames, the lateral walls are set on foundations of width B_F . Let us introduce the geometrical ratios that will be referred to later on. From Fig. 1, the overburden depth ratio is defined as D_0/L , the structure aspect ratio is L/H and the foundation ratio is B_F/L . The aspect ratios considered in the following analyses vary from 4 to $1/2$, the end values used principally as limit cases. In the case of rectangular structures with aspect ratios L/H of 2 or more, the horizontal elements are supported by vertical middle walls in such a way that the maximum horizontal length of unsupported span is no greater than H (thus, for example, with $L/H = 4$ there are 3 vertical connecting walls).

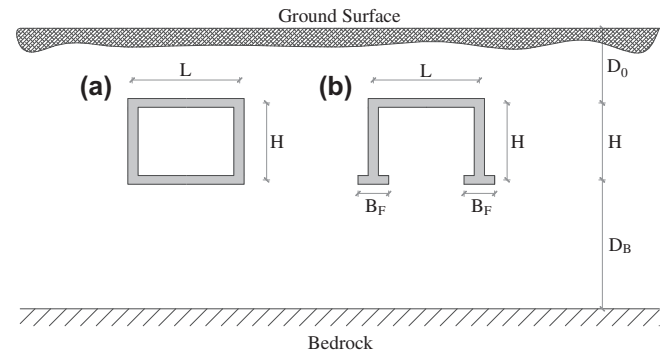


Fig. 1. Geometrical quantities characterizing the 4-sided rectangular structure (a), and the 3-sided rectangular structure (b).

2.2. Finite element model

The typical finite element meshes used for the pseudo-static and dynamic analyses of the free field condition and the soil–structure interaction are shown in Fig. 2. For all analyses, a single-phase medium was considered. For the soil–structure interaction analysis, the soil was discretized with nearly 3200 eight-node, linear-strain finite elements, while the structure was discretized with three-node beam elements. The non-linearity introduced by the frictional soil–structure interface meant that we could not take advantage of any symmetry of the problem, so the whole domain was considered. The total number of nodes was about 9860, with nearly 19,000 unknowns. At the soil–structure interface, the nodes can be perfectly tied (in the case of a *tied* interface) or a frictional interface is simulated with contact surfaces, allowing no penetration between the soil and the structure. To reduce numerical inaccuracies, the maximum aspect ratio adopted for the finite elements was 8:1; maximum values of 5:1 or 10:1 are typically recommended in the literature for this kind of element, the larger ratio being the limit for ensuring an accurate estimation of the nodal displacement (see Burnett, 1987).

The bottom boundary of the finite element mesh represents the bedrock and was assumed to be perfectly rigid and rough. Its depth (D_B of Fig. 1) was chosen to be greater than the maximum dimension of the box structure so that its effect is irrelevant on the response. The model included a portion of soil spanning to a horizontal distance about 58.0 m from the buried structure (in the case of $L/H = 1$, with $H = 4.0$ m), having established that any further extensions had negligible effects on the numerical results. In both the finite element meshes (Fig. 1a and b), and for both the pseudo-static and the dynamic analyses, the nodes on the vertical boundaries were constrained to have the same vertical and horizontal displacements. This kind of boundary condition was suggested by Zienkiewicz et al. (1988) for seismic problems and is called a *repeatable* boundary condition: it achieves exactly the same results as more complex methods (e.g. the silent boundary condition proposed by Lysmer and Kuhlemeyer (1969)), but more simply. Note that in the finite element mesh used for the free-field analyses (Fig. 2a), this boundary condition practically reduces the 2D problem to a 1D problem.

For the dynamic analyses, we imposed a horizontal acceleration history on the bedrock as in Fig. 3 (i.e. at the bottom boundary). This artificial accelerogram was generated to produce the same response spectra as the one used by Wang (1993), then scaled to obtain a peak acceleration a_g of 0.35 g, consistent with the value suggested by Eurocode 8 for highly seismic zones (CEN, 2004).

The load condition for the pseudo-static analyses consisted of a distributed horizontal volume force (Fig. 4), corresponding to the peak accelerations established from free-field analyses at the depth

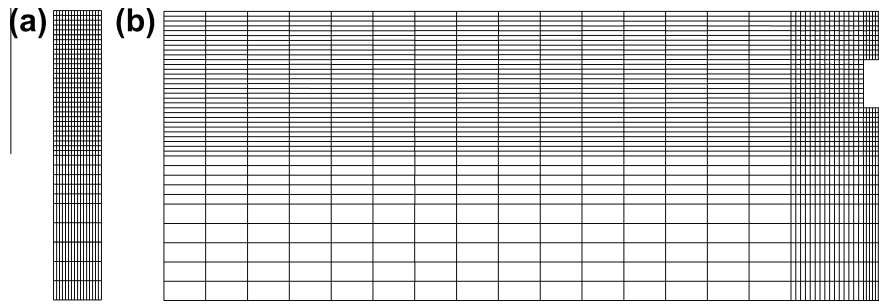


Fig. 2. Finite element mesh used for free-field analyses (a), and soil–structure interaction analyses (left-hand portion of the finite element mesh) (b).

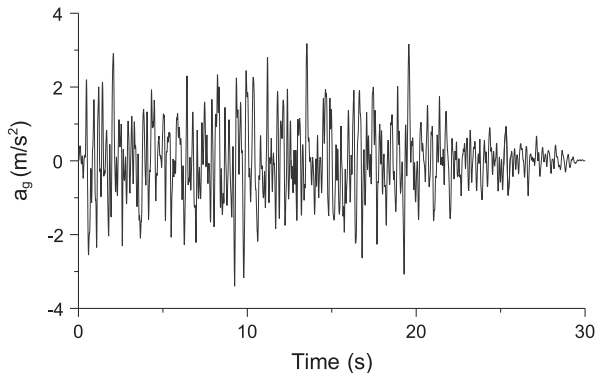


Fig. 3. Acceleration time history applied to the bedrock in dynamic analyses.

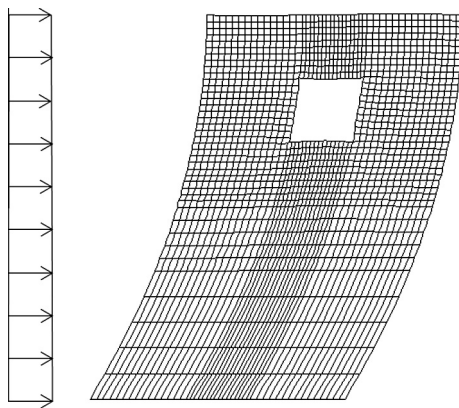


Fig. 4. Schematics of the volume force adopted for pseudo-static analyses.

of the buried structure. The amplification coefficient varies vis-à-vis the bedrock acceleration with the burying depth and bedrock depth, but for the most part in our dynamic analyses it was approximately 1.80. The pseudo-static analyses were thus performed with a horizontal volume force corresponding to the acceleration of $1.80 \times 0.35 \times g = 0.63 \times g$. Poisson's ratio was normally set at 0.33, though we performed some analyses to test the sensitivity of the response to Poisson's ratio, as explained in Section 4.4.

Both the structure and the soil were assumed to be linear elastic. Soil shear stiffness and soil damping were kept constant in the analyses, whereas the stiffness of the structure was changed by conventionally changing the Young's modulus of concrete to achieve bending stiffnesses of the box walls ranging between $14.4 \text{ MN m}^2/\text{m}$ and $7660.4 \text{ MN m}^2/\text{m}$ to explore the effects of the flexibility ratio. Clearly, this linear soil model does not account for any uneven stiffness degradation of the portion of soil surrounding the buried structure (Huo et al., 2006). As mentioned

earlier, this simplification may result in an over- or underestimation of the computed structure distortions, depending on the soil–structure stiffness rate.

Appropriate soil stiffness and damping values had to be selected for the dynamic analyses. Soil stiffness and damping depend on the strain amplitude, which in turn depends on the acceleration history and the damping itself. Soil stiffness and damping were assumed constant throughout the soil profile (consistently with Wang 1993; Anderson et al. 2008; Bobet et al. 2008; Huo 2005) and were selected from Seed et al. (1986), using an iterative procedure applied to the free-field analysis (Kramer, 1996) and considering the mean strain amplitude. For a maximum bedrock acceleration of $a_g \approx 0.35 g$, for instance, the selected damping value was 14%, while the constant soil shear stiffness was $G = 72 \text{ MPa}$. In all linear dynamic analyses, soil damping was assumed to follow Rayleigh's model. One drawback of Rayleigh damping is known to be its dependence on frequency. To overcome this problem, the two Rayleigh parameters were selected so as to obtain the target damping in a range of frequencies including the first two modes (which have modal participating masses of 81.1% and 9.0%, respectively, so they cover more than 90% of the total participating mass).

In the case of a frictional soil–structure interface and elastoplastic soil behavior, the initial stress condition in the soil is very important because the normal stress at the interface controls the maximum shear stress, according to the Mohr–Coulomb friction model. A friction ratio of $\mu = 0.35$ was chosen for the soil–structure interface in most analyses. We assumed an initial geostatic stress increasing linearly with depth, with a coefficient of earth pressure at rest $K_0 = 0.50$, this coefficient being the ratio of horizontal to vertical effective stress, $K_0 = \sigma_h/\sigma_v$. It is worth noting that the K_0 stress condition was only approximately satisfied along the vertical walls due to flexural deformations.

2.3. Definition of the response parameters

To correlate the results of this study with the existing literature, in the following sections we present the results of our analyses in the same format as in Wang (1993), i.e. in terms of relative racking stiffness R , versus flexibility ratio F . The flexibility ratio F is defined as the ratio of the shear stiffness of the soil element G to the racking stiffness of the structure, thus:

$$F = \frac{GL}{SH}, \quad (1)$$

where the stiffness S coincides with the concentrated force needed to cause a unit racking deflection of the structure (so the unit of S is kN/m^2). For a rectangular frame with an arbitrary configuration, the stiffness S can be calculated by means of a simple linear frame analysis. The geometry to consider in evaluating S was clearly defined by Wang (1993) for 4-sided rectangular tunnels (see Fig. 5a), while for 3-sided rectangular tunnels we propose the geometry shown in

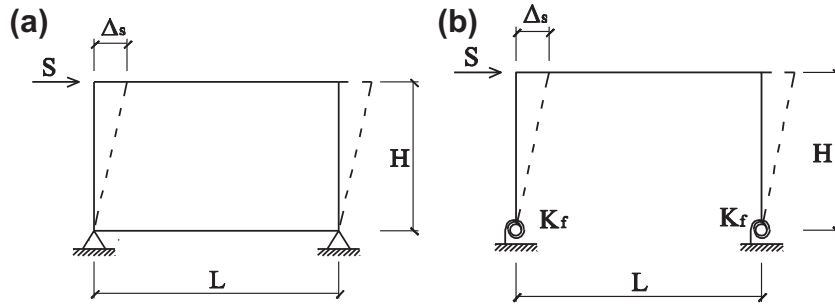


Fig. 5. Static schemes used to evaluate the racking stiffness of the structure in terms of the force S needed to cause a unit racking deflection of the 4-sided (a) and 3-sided (b) rectangular structures.

Fig. 5b, where the rotational stiffness of the shallow foundations, K_f is taken into account. K_f was calculated from the theory of elasticity according to the following expression, proposed by Poulos and Davis (1974):

$$K_f = \frac{2G}{1-\nu} B^2 L I_\theta, \quad (2)$$

where I_θ is a coefficient depending on the geometry and stiffness of the foundations, which is consequently known because it is calculated using the elasticity theory (and it is usually given in graphics or tables), ν is Poisson's ratio and G is the shear modulus of the soil, which coincides with the value adopted for the free-field analyses.

We must bear in mind that an implication of Wang's (1993) definition of the flexibility ratio is that for $F < 1$ the structure is stiffer than the surrounding ground ($F \rightarrow 0$ represents a perfectly rigid structure), while for $F > 1$ it is less stiff than the surrounding ground ($F \rightarrow \infty$ represents a perfectly flexible structure).

As typically done in the literature, we report the output of the analysis in terms of relative racking stiffness R (also denoted as the *racking coefficient* or *racking ratio*). This is given by the ratio of the racking distortion of the buried structure Δ_s , calculated by means of the pseudo-static or dynamic analysis on the finite element mesh of Fig. 2b, to the lateral shear deformation of the free field, Δ_{ff} (expressed as a length), calculated under the same pseudo-static or dynamic conditions on the *free field* finite element mesh of Fig. 2a, namely

$$R = \frac{\Delta_s}{\Delta_{ff}}. \quad (3)$$

When the structure's movement involves no rocking, as is typically the case of deeply-buried structures, Δ_s simply coincides with the difference between the top and bottom horizontal displacements of the frame (Δ_{TOT} in Fig. 6). On the other hand, we will see in the next section that shallow structures with a small aspect ratio can undergo significant rocking rotation γ_R . In this case, as shown in Fig. 6, Δ_{TOT} must be separated from the differential horizontal displacement $\Delta_R = H\gamma_R$ produced by rocking rotation, in order to deduce the net distortion of the frame:

$$\Delta_s = \Delta_{TOT} - \Delta_R. \quad (4)$$

Similarly to Eq. (3), we can define the ratios

$$R_R = \frac{\Delta_R}{\Delta_{ff}} \text{ and } R_{TOT} = \frac{\Delta_{TOT}}{\Delta_{ff}} \quad (5)$$

and the relationship between the three is evidently:

$$R = R_{TOT} - R_R. \quad (6)$$

Very often in the literature it is implicitly assumed that rocking is negligible, so the quantities R and R_{TOT} coincide (e.g. Wang 1993). In the present work, however, a distinction is necessary because it has become clear that rocking is not negligible under

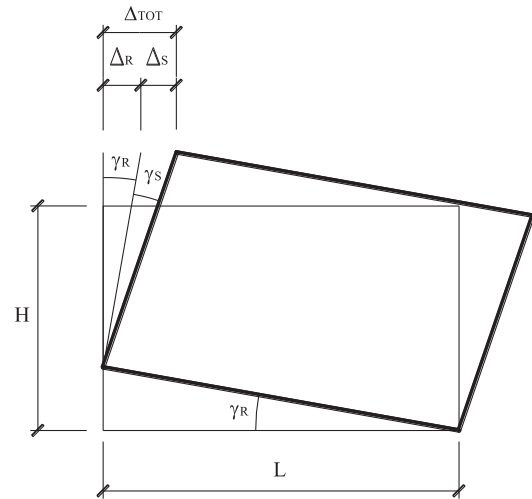


Fig. 6. Relationship between rocking rotation (γ_R), shear distortion (γ_S) and total differential displacement for a box structure.

certain conditions, discussed in the next Sections. The Appendix to this paper reports an estimation of the error incurred in evaluating the members' forces when R and R_{TOT} are confused.

3. Preliminary observations on the response of shallow-buried structures

Before proceeding with the parametric analysis, it is essential to narrow down the problem. In the following paragraphs, we highlight some points that help to clarify the physical nature of the problem, and thereby reduce the number of cases deserving further investigation. By using some representative examples, in Section 3.1 we first recall the justification for the validity of simplified analyses on deeply-buried structures. In contrast with these considerations, in Section 3.2 we analyze some typical features of the response of shallow-buried structures. In Section 3.3 we show that there is critical burial depth beyond which the depth D_{CO} no longer affects the structure's behavior, and we provide practical values for its estimation. In particular, the structure's behavior will be shown to change gradually with the burial depth, from the null to the critical depth D_{CO} , so these cases can be taken as extremes for estimating the response of a shallow-buried structure.

3.1. Features of the response of deeply-buried structures

In this paper, we are comparing shallow-buried structures with deeply-buried ones, so we must first clarify what we mean by the term 'deeply-buried'. Here, we define a structure as being

deeply-buried when the shear strength at the soil–structure interface is not fully mobilized, so there is negligible slip at the interface, which can therefore be considered as if it were fully tied. As a consequence, because the interface mechanism for deeply-buried structures is independent of the burial depth, the same is expected to apply to the racking coefficient R . It is implicit in the above definition that a structure at a given burial depth may be shallow- or deeply-buried depending on the intensity of a given earthquake.

Fig. 7a shows the results of the pseudo-static analyses performed, for different flexibility ratios F , on a deeply-buried rectangular box section with an aspect ratio $L/H = 1$, a peak ground acceleration at the bedrock $a_g = 0.35$ g, and a bedrock depth ratio $D_B/L = 4$. More specifically, the overburden depth ratio was $D_0/L = 1$, which is large enough for a deeply-buried condition (i.e. any further increase in depth would not appreciably change the results), as we demonstrate in Section 3.3. The graph clearly shows, as expected, that the response is virtually independent of the interface's behavior (fully tied or frictional with $\mu = 0.35$), since the scatter between the corresponding racking coefficients R is negligible.

The graph in Fig. 7b shows the results for a 3-sided rectangular structure with symmetrical foundations and a foundation ratio $B_F/L = 0.375$ (corresponding to $B_F = 1.50$ m and $L = 4.0$ m). Here again, we see that the response is independent of the interface mechanism assumed. Comparing the two graphs we also see that the curves obtained for the 4-sided and 3-sided structures almost overlap. Without reporting the results of other analyses, we can see that this result is no coincidence, but holds true for any geometrical configuration tested, providing the structure is deeply buried. In other words, if the rotational stiffness K_F of the shallow foundations is duly taken into account in the evaluation of F (as explained in Section 2.3), deeply-buried 3-sided rectangular structures behave in the same way as 4-sided structures with the same flexibility ratio F .

These results, and particularly those obtained for the 4-sided box sections, are fully consistent with those reported elsewhere in the technical literature. Fig. 8 draws a comparison between the racking response obtained for 4-sided deeply-buried structures with various flexibility ratios F and aspect ratios L/H , and the numerical results obtained by Wang (1993), and the analytical results reported by Huo et al. (2006), both achieved in deeply-buried conditions. Not surprisingly, we see that our results essentially match with Wang's numerical solutions. Our analysis also shows that, given a specific F , the racking response R increases slightly

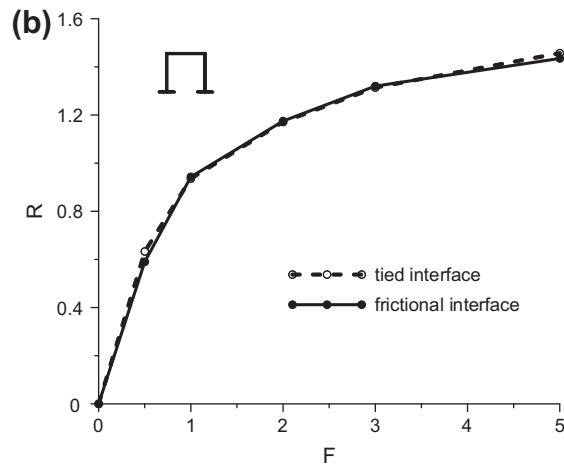
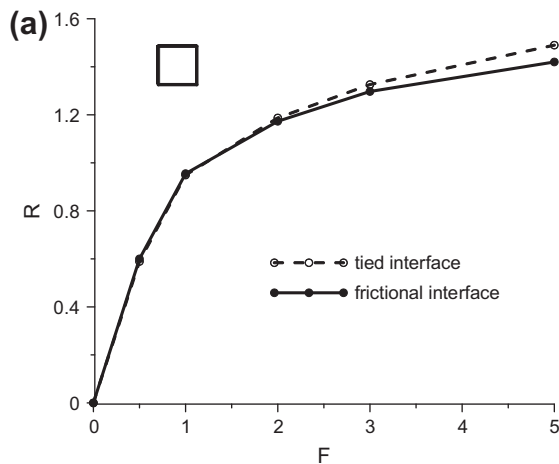


Fig. 7. Racking ratio R versus flexibility ratio F of deeply-buried (depth ratio $D_0/L = 1$), 4-sided (a) and 3-sided (b) rectangular structures (where $L/H = 1$) with tied and frictional soil–structure interfaces.

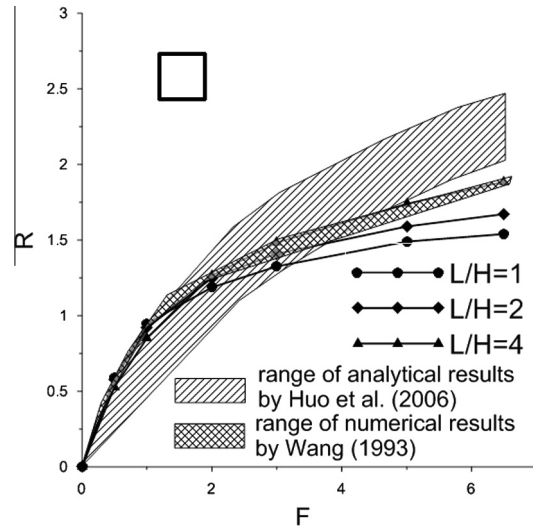


Fig. 8. The racking ratio R calculated in the present study for deeply-buried, 4-sided rectangular structures compared with previous reports from Wang (1993) and Huo et al. (2006).

with the aspect ratio L/H , as in the prediction of the closed form solution proposed by Huo et al. (2006).

Though they are not shown here for the sake of brevity, we also carried out dynamic analyses, which confirmed that pseudo-static and dynamic analyses generate virtually identical results in terms of the racking coefficient R . It is worth noting that this observation is consistent with the common opinion that dynamic amplification is negligible as long as the wavelength is greater than the dimension of the opening (Hendron and Fernández, 1983).

3.2. Particular aspects of a shallow-buried structure's behavior

Judging from our analyses, shallow-buried structures reveal some unexpected, particular features in their interaction with the surrounding soil, which can be summarized as follows: the importance of non-linearity (introduced by frictional soil–structure interface); the possibility of the whole buried structure rocking, which may even result in the partialization of the base foundations; and the possibility of soil detachment from the vertical walls. These aspects of the soil–structure interaction are fairly

reasonable from a physical standpoint, but had never been emphasized before, probably because they are scarcely evident (or not at all) from conventional, linear-elastic analyses. Such interactions obviously depend on the amount of seismic acceleration. These particular aspects are briefly recalled below.

As might be reasonably expected, the effects of frictional nonlinearities become particularly important in shallow-buried structures due to the low stress level. This is apparent in the case of the frictional soil–structure interface in Fig. 9, where the behavior of two 4-sided rectangular structures with $L/H = 1$ and $F = 1$ (Fig. 9a) and $L/H = 4$ and $F = 3$ (Fig. 9b) is considered for different burial depths. The results in Fig. 9 clearly show that the difference in terms of R_{TOT} between tied and frictional soil–structure interfaces gradually changes from the condition of deep burial depth ($D_0/L = 1$, at which the R_{TOT} values obtained with tied and frictional interfaces coincide with each other) to the condition of null burial depth ($D_0/L = 0$ at which the R_{TOT} values obtained with tied and frictional interfaces differ considerably from one another). Note in Fig. 9 that friction at the interface may lead to either an increase or a decrease in the value of R_{TOT} vis-à-vis the tied condition, depending on the aspect ratio L/H and the flexibility ratio F . The results shown in Fig. 9 consequently emphasize the importance of taking non-linear frictional effects at soil structure interface properly into account in the analysis of shallow-buried structures.

A further important aspect of a shallow structure's behavior is rocking. Here again, it is fairly reasonable to expect shallow-buried, stiff structures with low aspect ratios L/H , to be affected by a rigid rotation (rocking), which may even lead to a partialization of the base foundation, as shown in Fig. 10a. It comes somewhat as a surprise, on the other hand, that rocking may be non-negligible with tied soil–structure interfaces at non-negligible burial depths, as we shall see below. Rocking is therefore enhanced by non-linear frictional effects at shallow burial depths, but may occur even with a linear behavior. Rocking obviously diminishes at lower peak accelerations, with decreasing structure stiffness values (i.e. with increasing flexibility ratio F) and increasing aspect ratios L/H (as we shall see in detail in Subsections 3.3).

Fig. 11 shows the total ratio R_{TOT} and the racking fraction R in relation to the flexibility ratio F and the depth ratio D_0/L , where $L/H = 1/2$, for both frictional (Fig. 11a and b) and tied (Fig. 11c and d) soil–structure interfaces. Rigid structures (with a small F) that have small aspect ratios ($L/H < 1$) are clearly the most affected by rocking, which gradually decreases with increasing overburden depths. As mentioned previously, non-null rocking occurs even at

non-negligible overburden depths in the case of a frictional interface, whereas (for the example shown in Fig. 11) rocking soon decreases with increasing overburden depths in the case of a tied interface.

It is worth adding that rocking in 3-sided rectangular structures with symmetrical foundations is much more limited than in 4-sided structures, due to the stabilizing effect of the slabs on the outside of the shallow footings.

The last particular aspect of the behavior of shallow-buried structures is soil detachment, which may occur when these structures are stiffer than the surrounding ground (i.e. with flexibility ratios $F < 1$), with large aspect ratios L/H and a frictional soil–structure interface. This is shown for the null overburden depth $D_0/L = 0$ in Fig. 10b, where the soil apparently becomes detached from the vertical walls of the rectangular structure. Soil detachment from the vertical walls is obviously meaningless in cohesionless soil (it could occur only in cemented soils or undrained clays) and in our calculations it is due to the assumption of a perfectly elastic soil response. From a physical standpoint, however, the soil pressure cannot be smaller than the active earth pressure or larger than the passive earth pressure, both evaluated under dynamic conditions (according to the method proposed by Mononobe and Okabe (e.g. Das, 1983), for instance). In our computations, soil pressure was never higher than the passive earth pressure under dynamic conditions, while the soil pressure calculated where soil detachment occurs is obviously smaller than the active soil pressure (Fig. 10b). In the cases of soil detachment, the calculated racking distortions of the structure (and consequently the member forces) can be expected to be greater than the actual distortions because the actual, non-null, active soil pressure along the vertical wall would lead to smaller distortions than the calculated null soil pressure (due to soil detachment). The simplified analyses presented in this work can therefore be expected to provide conservative assessments of the racking ratio R in cohesionless soils, when soil detachment occurs in the simulations.

3.3. Critical burial depth

The two kinds of behavior of the soil–structure interface (perfectly tied or frictional with some sliding) should be seen not as alternatives, but as the two limit cases of a continuous range of behaviors depending on the peak acceleration applied. Within this range, the soil–structure interface is obviously expected to behave as if it were perfectly tied for the smallest peak accelerations,

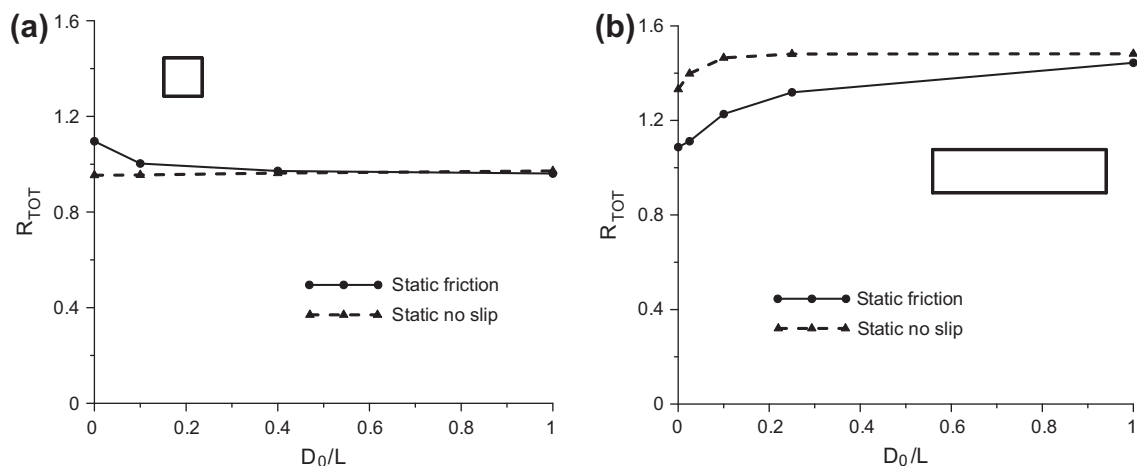


Fig. 9. Racking ratio R_{TOT} versus flexibility ratio F of shallow-buried (depth ratio in the range $D_0/L = 0$ and $D_0/L = 1$), 4-sided rectangular structures, where $L/H = 1$ and $F = 1$ (a) and $L/H = 4$ and $F = 3$ (b).

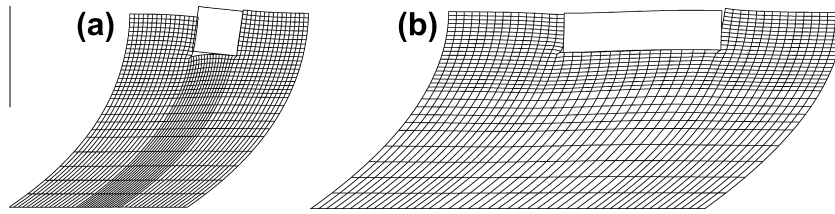


Fig. 10. Deformed configuration (central portion of FE mesh) for 4-sided stiff ($F = 0.5$) rectangular structures, with a frictional soil–structure interface and a null depth ratio $D_0/L = 0$, where $L/H = 1$ (a) and $L/H = 4$ (b).

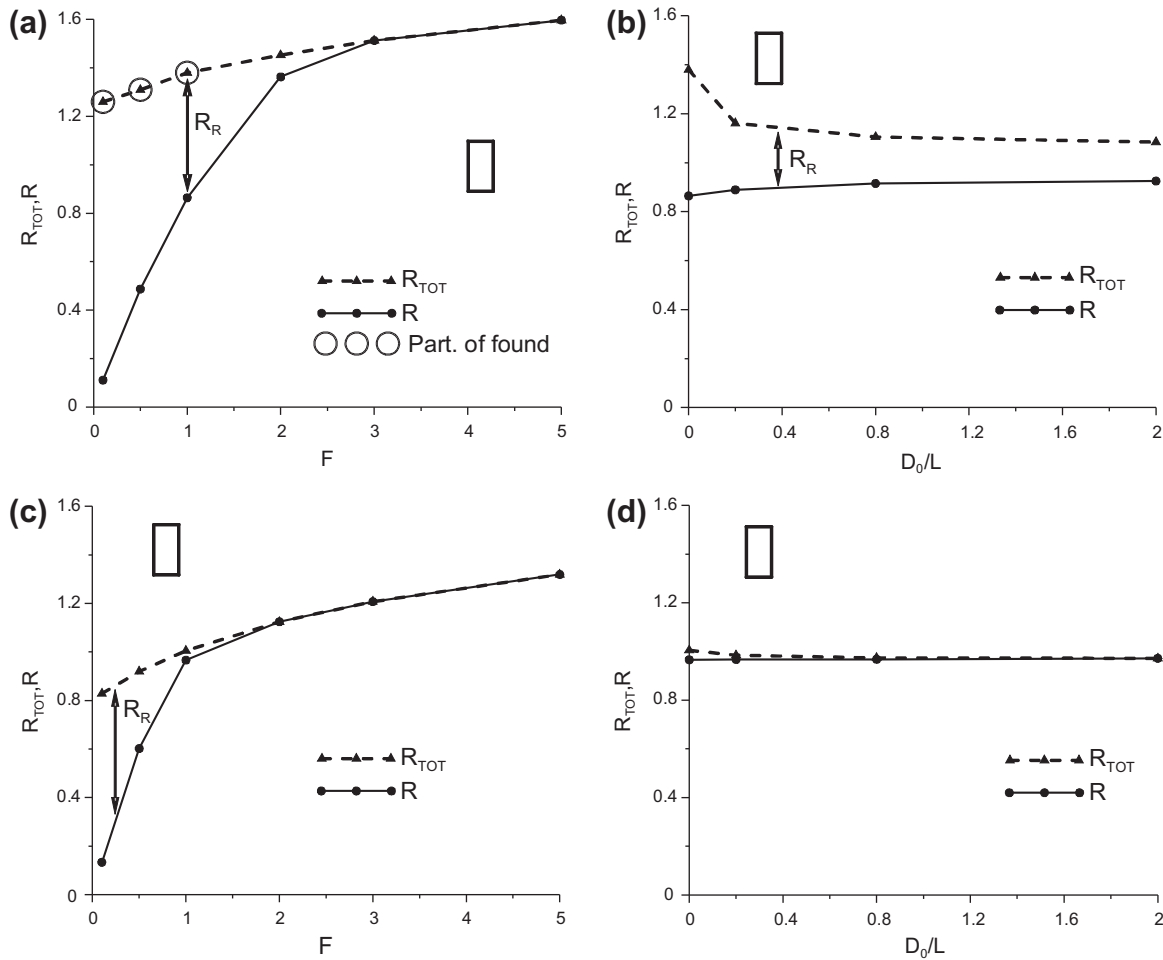


Fig. 11. Racking ratios R_{TOT} and R of 4-sided rectangular structures, where $L/H = 1/2$ versus: (a) the flexibility ratio F with frictional soil–structure interfaces (for null depth ratio $D_0/L = 0$); (b) the depth ratio D_0/L with frictional soil–structure interfaces (for $F = 1$); (c) the flexibility ratio F with tied soil–structure interfaces (for null depth ratio $D_0/L = 0$); and (d) the depth ratio with tied soil–structure interfaces (for $F = 1$).

whereas it may be subjected to considerable sliding (even leading to rocking) for the largest peak accelerations.

We can infer from Fig. 9 that the burial depth ratio D_0 does not affect the structural response beyond a certain critical value D_{C0} , where the frictional soil–structure interface has a perfectly tied behavior.

To establish an order of magnitude for said critical depth ratio D_{C0}/L , some analyses were performed using different values for D_0/L and L/H . The critical depth ratio D_{C0}/L is defined here as the depth ratio above which the R values calculated with frictional and tied soil–structure interfaces differ from one another by less than 5%. Fig. 12 shows the critical depth ratio D_{C0}/L in relation to the aspect ratio L/H , for different flexibility ratios F , maximum soil accelerations a_{max} and friction ratios μ . We can see that the critical

depth ratio D_{C0}/L increases with the aspect ratio L/H , whereas a decrease in the friction ratio μ or an increase in the peak soil acceleration a_{max} considerably increases the critical depth ratio D_{C0}/L . The critical depth ratio D_{C0}/L also decreases with an increase in the flexibility ratio F , meaning that flexible structures are less affected by the non-linearities at shallow depths than stiff structures.

4. Parametric analysis of null overburden structures

In the previous section we demonstrated that the burial depth does not affect the structural response beyond a certain critical depth D_{C0} , where the frictional soil–structure interface has a perfectly tied behavior. We also saw that, above this depth, the

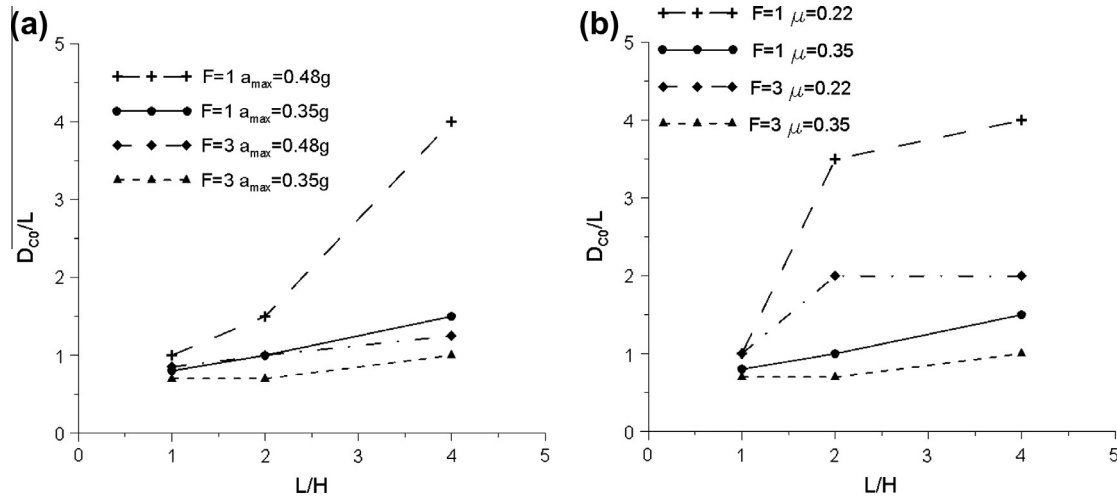


Fig. 12. Critical depth ratio D_{co}/H versus aspect ratio L/H , for 4-sided rectangular structures with different flexibility ratios F : effects of peak soil acceleration (a) and friction ratio μ . (b).

predicted response is sensitive to the assumptions concerning the interface’s behavior, which is usually uncertain at the design stage. With a view to providing useful, practical design tools, we concentrate on the case of a null overburden depth, $D_0/L = 0$ because this coincides with the limit situation. In particular, the roles of the structure’s geometry, the peak acceleration and the flexibility ratio are examined in more detail.

4.1. Effects of the flexibility ratio

This Subsection examines the effects of the flexibility ratio F (ranging between 0 and 5) for different values of the aspect ratio L/H (ranging between the two extreme cases of $L/H = 0.5$ and $L/H = 4$) on shallow-buried rectangular structures ($D_0/L = 0$).

The results for 4-sided and 3-sided rectangular structures are shown in Figs. 13 and 14, respectively. For the 3-sided rectangular structures (Fig. 14), we assumed that $B_f/L = 0.375$. In Fig. 13 special symbols are used to highlight the partialization of the base foundation and soil detachment. The results shown in Figs. 13 and 14 prompt the following observations:

(a) for both 4-sided and 3-sided, shallow-buried rectangular structures with tied interfaces (Figs. 13a and 14a), the aspect ratio L/H has much the same effects as in deeply-buried structures;

(b) the aspect ratio L/H is comparatively more important for frictional soil–structure interfaces, due to the non-linear effects induced by the shallow depths: in particular, the larger the structure aspect ratio L/H , the smaller the R (Figs. 13b and 14b);

(c) for 4-sided rectangular structures (Fig. 13) with $L/H \leq 2$, the racking ratio R obtained with a frictional interface comes close to the one obtained with a tied interface; with $L/H > 2$, on the other hand, the racking ratio R obtained with a frictional interface is always smaller than the one obtained with a tied interface;

(d) for flexibility ratios higher than around $F > 3$, and especially for $L/H < 1$, the 4-sided and 3-sided rectangular structures are so flexible that any further decrease in stiffness (or increase in F) has little effect and the racking ratio remains approximately constant;

(e) rocking occurs in buried 4-sided rectangular structures with $L/H < 1$, particularly in the range of $F < 1$ (Fig. 13b).

4.2. Effect of the structure’s geometry

To better illustrate the effects of the aspect ratio on shallow-buried structures, Figs. 15 and 16 again plot the results shown in Figs. 13 and 14, but this time as a function of L/H , and for flexibility

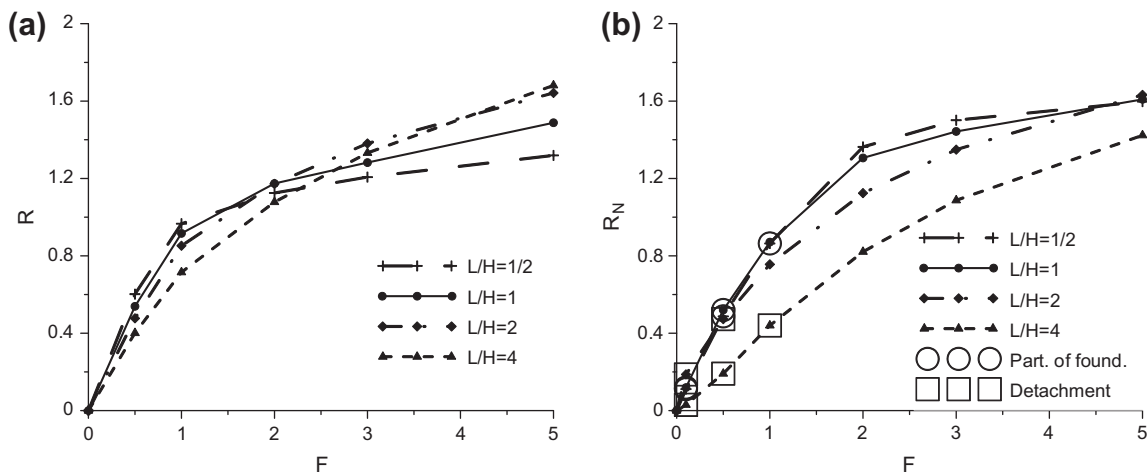


Fig. 13. Racking ratio R versus flexibility ratio F of shallow-buried (depth ratio $D_0/L = 0$), 4-sided rectangular structures, with tied (a) and frictional (b) soil–structure interfaces.

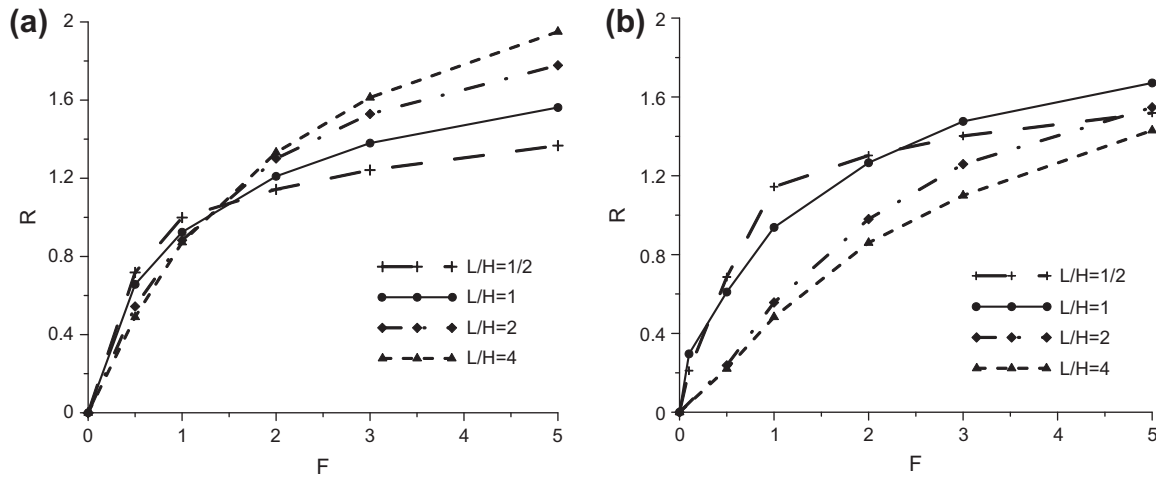


Fig. 14. Racking ratio R versus flexibility ratio F of shallow-buried (depth ratio $D_0/L = 0$), 3-sided rectangular structures with conventional shallow foundations, with tied (a) and frictional (b) soil–structure interfaces.

ratios of $F = 1$ and $F = 3$ (while keeping $D_0/L = 0$, $D_B/H = 4$ and, for the 3-sided rectangular structures, $B_F/L = 0.375$, as before). We can immediately see that:

- (a) the aspect ratio L/H scarcely affects the null overburden behavior of 4-sided rectangular structures with tied soil–structure interfaces (Fig. 15a), while larger differences are associated with frictional soil–structure interfaces (Fig. 15b);
- (b) the behavior of shallow-buried, 3-sided rectangular structures with frictional soil–structure interfaces is more deeply affected by their aspect ratio L/H (Fig. 16b); in particular, the racking ratio R is higher the lower the aspect ratio L/H and the higher the flexibility ratio F (or the more the structure is flexible by comparison with the surrounding soil).

As noted previously, for rigid ($F < 1$), 4-sided structures with small aspect ratios ($L/H \approx 0.5–1.0$), racking results in a partialization of the base foundation for the peak accelerations considered here.

4.3. Effect of maximum accelerations on shallow-buried rectangular structures

As seen in Subsection 3.3, the seismic behavior of shallow-buried rectangular structures under increasing peak accelerations can be expected to shift from the case of a perfectly tied interface to the case of a sliding frictional interface. This effect is particularly relevant for shallow-buried rectangular structures because – given the low soil overburden – sliding at the soil–structure interface occurs even when very small accelerations are applied. Fig. 17 shows the results obtained with a pseudo-static analysis performed with different volume forces (corresponding to different maximum accelerations) on 4-sided, shallow-buried rectangular structures (depth ratio $D_0/L = 0$) with flexibility ratios of $F = 1$ and $F = 3$, for a unit aspect ratio ($L/H = 1$). For the sake of completeness, we extended our analyses to a range of peak accelerations beyond the maximum design values provided by most seismic codes. It is worth emphasizing that, with a perfectly tied soil–structure interface, the racking ratio R is unaffected by the maximum soil acceleration because the problem is linear. Note that, within the limit

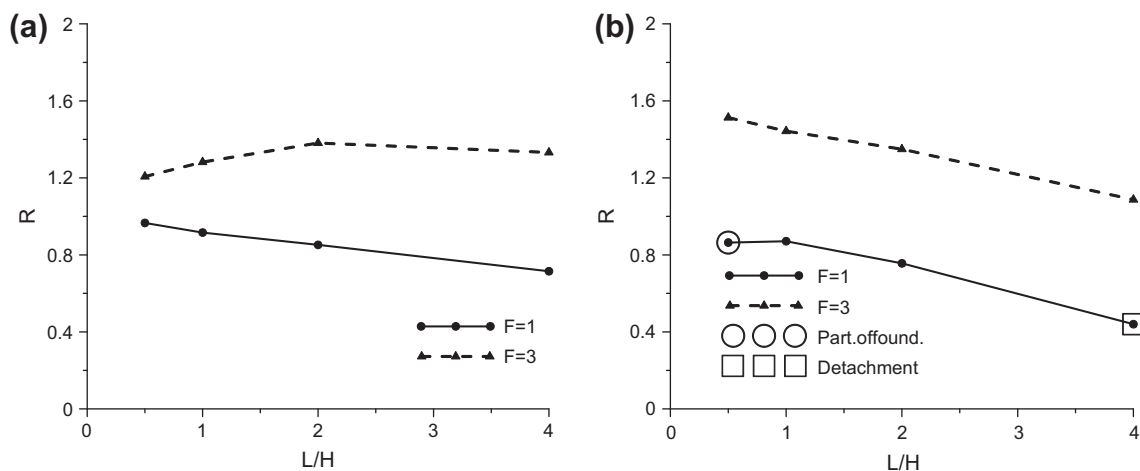


Fig. 15. Variations in the racking ratio R with the aspect ratio L/H , for shallow-buried (depth ratio $D_0/L = 0$), 4-sided rectangular structures with tied (a) and frictional (b) soil–structure interfaces.

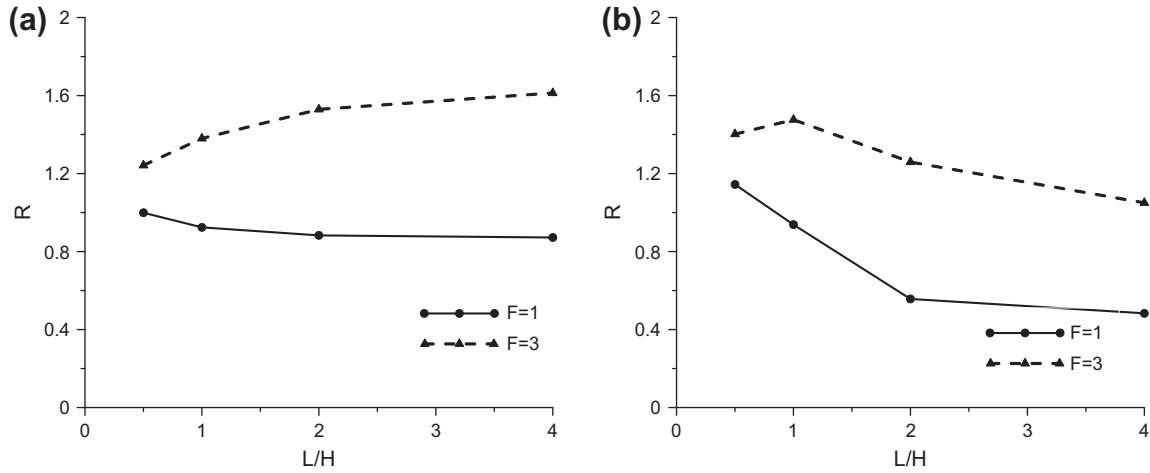


Fig. 16. Variations in the racking ratio R with the aspect ratio L/H , for shallow-buried (depth ratio $D_0/L = 0$), 3-sided rectangular structures with tied (a) and frictional (b) soil-structure interfaces.

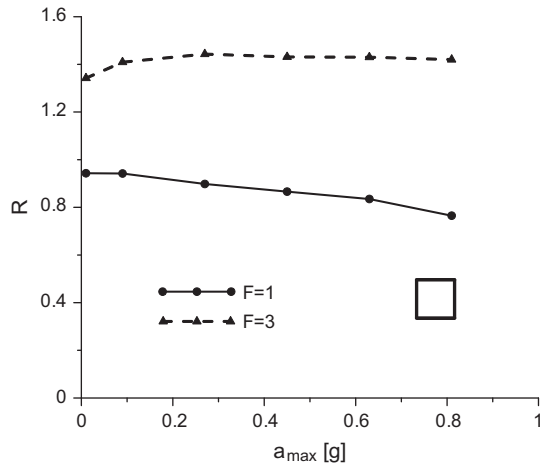


Fig. 17. Variations in the racking ratio R with maximum soil acceleration a_{max} , for shallow-buried, 4-sided rectangular structures with $F = 1$ and $F = 3$, $L/H = 1$ (depth ratio $D_0/L = 0$), with frictional soil-structure interfaces.

of $a_{max} \rightarrow 0$, the racking ratio R obtained with the frictional interface nears the value obtained with the tied interface (as expected), as shown in Fig. 17.

As can be inferred from Fig. 17 as well, for a given maximum acceleration, the stiffness of the structure affects the response of the frictional soil-structure interface. In particular, the higher the value of F (i.e. the more the structure is flexible), the more a frictional interface tends to behave like a tied interface, with negligible sliding. Particularly when the flexibility ratio F is 3 or higher, the response is basically independent of the peak soil acceleration, whereas for $F = 1$ the structural response decreases with the maximum soil acceleration a_{max} .

4.4. Effects of non-homogeneous soil stiffness and Poisson's ratio

The results obtained in the case of non-homogeneous soil stiffness are not reported here for the sake of brevity, but the general outcome was that a soil stiffness increasing proportionally to the square root of the mean in situ effective stress generates much the same results (in terms of the racking ratio R) as a homogeneous soil stiffness with increasing depth (for $H = 4.0$ m), providing the mean shear stiffness of the soil surrounding the structure is used to assess the flexibility ratio F .

We also performed some analyses to investigate the role of a Poisson's ratio in the range of 0.10–0.495. The effects of Poisson's

ratio are not shown here because we found that, for a 4-sided rectangular structure (with a unit aspect ratio of $L/H = 1$, a null depth ratio of $D_0/L = 0$, a unit flexibility ratio $F = 1$, and a frictional soil-structure interface), the racking coefficient R decreases for higher Poisson's ratios and flexibility ratios F , following the general trend reported by Penzien (2000), who only considered tied soil-structure interfaces.

4.5. Practical design rules

We can summarize the main findings of the analyses reported in the previous sections as follows:

- (a) beyond a critical burial depth D_{CO} , response is independent of burial depth, and the interface's behavior can be assumed to be tied;
- (b) the critical burial depth D_{CO} depends on the friction ratio μ and on the earthquake's intensity; assuming a friction ratio no lower than $\mu = 0.35$ and a maximum soil acceleration no greater than $a_{max} = 0.48$ g, this critical depth is comparable to the maximum dimension L in the structure (see Subsection 3.3);
- (c) with overburden changing from D_{CO} to zero, the behavior of a shallow-buried structure gradually changes from the deep burial condition ($D_0 > D_{CO}$) to the null overburden condition (see Subsection 3.2); thus deep and null overburden conditions can be taken as limits of the response estimate;
- (d) at the null overburden depth, response is sensitive to what happens at the tied or frictional interface: depending on the flexibility ratio, the tied condition may be considered as an upper- or lower-bound estimate (see Subsection 4.1);

With a view to providing a practical design tool for estimating the seismic response of shallow-buried structures, we studied 8 different geometrical configurations and, for each of them, Fig. 18 shows the relationship between racking ratio R and flexibility ratio F under three conditions: deeply buried; zero overburden with tied interface; zero overburden with frictional interface and $\mu = 0.35$. For a practical use of these charts, it should be noted that:

- (a) there is a flexibility ratio F_0 below which the deeply-buried condition provides the most critical value of R (e.g. $F_0 = 2$ for 3-sided boxes with $H/L = 2$, Fig. 18g); thus, when $F \leq F_0$, the deeply-buried solution can be seen as a conservative solution for shallow-buried structures;

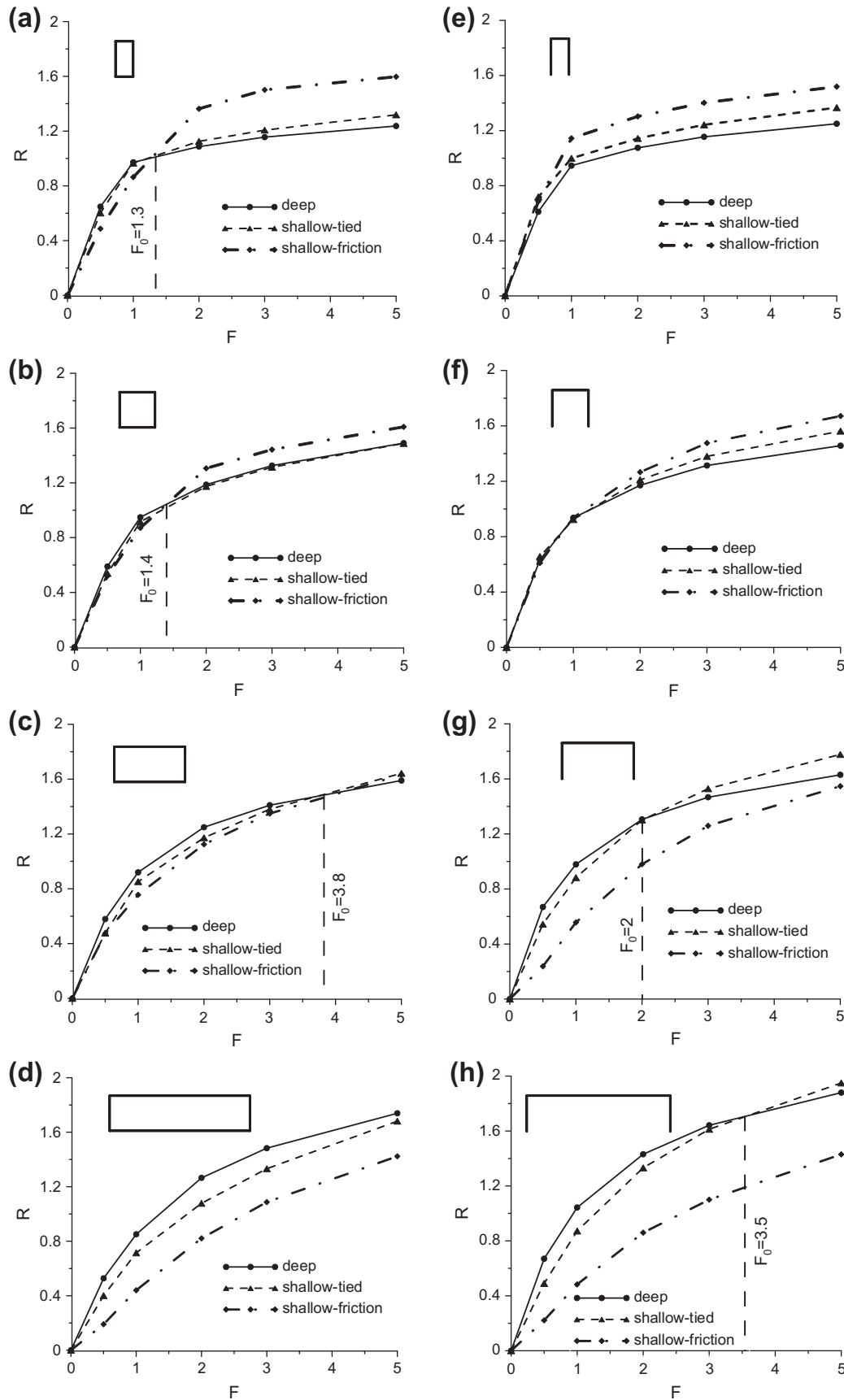


Fig. 18. Racking ratio R versus flexibility ratio F for different geometrical configurations (4- and 3-sided structures, L/H varying from $1/2$ to 4), assuming a deep burial depth and a null overburden depth: L/H equal to $1/2$ (a and e); 1 (b and f); 2 (c and g) and 4 (d and h).

(b) for $F > F_0$, the null-overburden solution is more critical than the deeply-buried one, and there are two different cases to consider:

1. When $L/H \geq 2$, the tied interface solution is an upper-bound estimate of the racking response; in this case, the null overburden, tied solution can be taken as a conservative estimate of the response.
2. When $L/H < 2$, the frictional model is more critical than the tied model; in this case, it is best to use the simplified solution only as a first approximation in the pre-design stage, and to be careful in selecting a meaningful value for the friction ratio.

The practical use of these charts is illustrated with the following examples.

Example 1. Let us assume a 3-sided, rectangular structure with an aspect ratio $L/H = 2$, a flexibility ratio $F = 1$, and a burial depth $D_0/L = 0.5$. As explained earlier, we can expect an intermediate response between the deeply-buried and the zero-overburden conditions. From the chart in Fig. 18g we infer that the racking ratio is $R = 0.98$ in the deeply-buried condition; we can also see that the tied interface model provides an upper-bound estimation of the zero-overburden condition, with $R = 0.88$, which is very close to the value in the deeply-buried condition. In this case, therefore, $R = 0.98$ can be taken as an acceptable and conservative estimation. If we now assume the same geometrical conditions and burial depth, but with $F = 3$, we can use the same chart to estimate $R = 1.46$ for the deeply-buried condition, and $R = 1.53$ for the zero-overburden condition in the worst case (tied interface). In this case, the burial depth being $D_0/L = 0.5$, we can take the mean value of the two, $R = 1.50$, as a first approximation, or we can simply take the upper-bound value $R = 1.53$ if we are looking for a conservative estimate.

Example 2. Let us assume a 4-sided square box ($L/H = 1$) again buried at $D_0/L = 0.5$. For $F = 1$, we can reason exactly as in example 1, and conservatively choose the solution for the deeply-buried condition, $R = 0.95$. For $F = 3$, the deeply-buried condition gives us $R = 1.33$, while the null-overburden solution ranges between $R = 1.32$ for the tied interface and $R = 1.44$ for the frictional interface (with $\mu = 0.35$). Since the tied interface is a lower-bound estimate in this case, we have to be careful in selecting a meaningful value for the friction ratio.

It is worth recalling that Bobet et al. (2008) suggested that Huo's results for deeply-buried structures can be used as an acceptable approximation for shallow-buried structures too. Their justification for this suggestion lay in the observation that the effect of a tied interface (corresponding to an underestimation of about 5–10%) compensates for the effect of a great overburden depth (roughly corresponding to a 15–20% overestimation). Examining Fig. 18 suggests that this approximation is reasonable, except in the case of flexible structures ($F > F_0$) with low aspect ratios ($L/H < 2$).

5. Conclusions

We investigated the scope and limits of the *simplified* methods used to estimate seismic response in shallow-buried rectangular structures. Our analysis was conducted mainly on the strength of pseudo-static finite element analyses, accounting for the effects of the type of soil–structure interface, the geometry of the box structure and the overburden depth, the maximum ground acceleration, and soil stiffness increasing with depth. Our findings enabled us to draw the following conclusions:

(a) for very deeply-buried structures, the soil–structure interface acts as if it were perfectly tied, so 4-sided and 3-sided rectangular structures behave in much the same way and the aspect ratio L/H has little effect;

- (b) non-linear effects (due to frictional soil–structure interface) are important in shallow-buried structures even at relatively small peak accelerations, unlike the situation in deeply-buried structures;
- (c) shallow-buried structures can behave in particular ways, e.g. rocking, partialization of base foundation, and soil detachment;
- (d) rocking must be accurately accounted for when calculating the member forces from racking deformations;
- (e) beyond a critical burial depth, D_{CO} response is independent of burial depth, and the interface's behavior can be assumed to be tied; under certain conditions (stated in Section 3.3), this critical depth, D_{CO} is comparable with the maximum dimension L of the box;
- (f) the behavior of a shallow-buried structure (i.e. with an overburden depth ranging between zero and D_{CO}) gradually changes from the deeply-buried condition ($D_0 > D_{CO}$) to the null-overburden condition, so these two conditions can be taken as the limits when estimating its response;
- (g) there is a value for the flexibility ratio F_0 below which the deeply-buried condition produces the most critical value of R ;
- (h) for $F > F_0$, and $L/H < 2$, the null overburden condition with a frictional interface is the most critical, so a careful evaluation of the role of friction is recommended.

Acknowledgments

Financial support from University of Trento is gratefully acknowledged. Special thanks go to Mrs. F. Bortot for her help in performing the numerical simulations and preparing the figures.

Appendix A.

The aim of this Appendix is to identify an order of magnitude for the error in the calculation of the member forces from the racking coefficient R , as proposed in this work. A simplified procedure for estimating the stress induced by seismic action on buried structural members was originally suggested by Wang (1993): first the lateral shear deformation of the free field, Δ_{ff} , is estimated by analyzing a vertically propagating shear wave; then the racking coefficient R is calculated from the flexibility ratio F , using the design plots given in Section 3; the seismically-induced racking deformation Δ_s is calculated from Eq. (3), namely:

$$\Delta_s = R\Delta_{ff}, \quad (7)$$

then the seismically-induced member forces can be obtained by means of a simple structural analysis on the rectangular frame with the geometry and load condition shown in Fig. 19, which undergoes the racking distortion Δ_s of Eq. (4). In detail, Wang suggested two separate load conditions (Fig. 19): a pseudo-concentrated force for deep-buried tunnels, and a pseudo-triangular pressure for shallow-buried tunnels. The static scheme for 4-sided and 3-sided structures is given in Fig. 5. In this Appendix, the seismically-induced member forces, assessed using linear and non-linear pseudo-static finite element analyses (which give results that practically coincide with those of dynamic analyses), are compared with those obtained using the simplified approaches based on the pseudo-concentrated force and the pseudo-triangular pressure proposed by Wang (1993), as shown in Fig. 19. This comparison is needed to calculate the range of the error affecting the estimation of the member moments in the cases of a null overburden depth and a frictional soil–structure interface considered in this work.

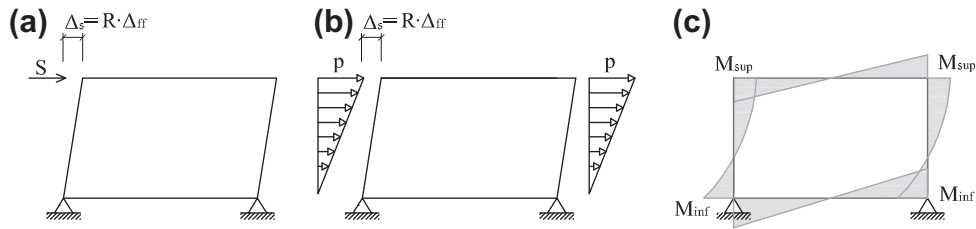


Fig. 19. Simplified frame analysis proposed by Wang (1993) for evaluating member forces: pseudo-concentrated force for deeply-buried tunnels (a), pseudo-triangular pressure for shallow-buried tunnels (b), convention adopted for denoting the bending moments (c).

Table 1
Comparison between maximum bending moments obtained with pseudo-static finite element analysis and simplified approaches based on the pseudo-triangular pressure and the pseudo-concentrated force (proposed by Wang, 1993, and shown in Fig. 19), for 4-sided rectangular structures (see Fig. 19c for the meaning of M_{sup} and M_{inf}).

		Pseudo-triangular pressure		Pseudo-concentrated force	
		M_{inf}/M_{inf}^{fem}	M_{sup}/M_{sup}^{fem}	M_{inf}/M_{inf}^{fem}	M_{sup}/M_{sup}^{fem}
$D_0/L = 1, F = 1, L/H = 1$	$\mu = 0.35$	1.16	0.93	1.00	1.18
	Tied	1.16	0.93	1.01	1.18
$D_0/L = 0, F = 1, L/H = 1$	$\mu = 0.35$	1.10	1.06	0.95	1.34
	Tied	1.17	1.13	1.01	1.42
$D_0/L = 0, F = 3, L/H = 1$	$\mu = 0.35$	0.95	0.89	0.80	1.09
	Tied	0.67	0.84	0.58	1.06
$D_0/L = 8, F = 1, L/H = 2$	$\mu = 0.35$	1.11	0.83	0.99	0.99
	Tied	1.19	0.89	1.06	1.06
$D_0/L = 0, F = 1, L/H = 2$	$\mu = 0.35$	1.09	0.97	0.96	1.16
	Tied	1.05	1.08	0.93	1.29
$D_0/L = 0, F = 2, L/H = 4$	$\mu = 0.35$	0.85	0.79	0.78	0.89
	Tied	0.85	0.98	1.11	0.77

Table 2
Comparison between the maximum member moments obtained with pseudo-static finite element analysis and the simplified approaches based on the pseudo-triangular pressure and the pseudo-concentrated force (proposed by Wang, 1993, and shown in Fig. 19), for 3-sided rectangular structures (see Fig. 19c for the meaning of M_{sup} and M_{inf}).

		Pseudo-triangular pressure		Pseudo-concentrated force	
		M_{inf}/M_{inf}^{fem}	M_{sup}/M_{sup}^{fem}	M_{inf}/M_{inf}^{fem}	M_{sup}/M_{sup}^{fem}
$D_0/L = 1, F = 1, L/H = 1$	$\mu = 0.35$	0.78	0.79	0.73	0.91
	Tied	0.96	0.82	0.90	0.96
$D_0/L = 0, F = 1, L/H = 1$	$\mu = 0.35$	0.74	0.72	0.70	0.85
	Tied	0.88	0.85	0.81	1.00
$D_0/L = 8, F = 1, L/H = 2$	$\mu = 0.35$	1.21	0.76	1.04	0.89
	Tied	1.29	0.80	1.17	0.94
$D_0/L = 0, F = 1, L/H = 2$	$\mu = 0.35$	0.83	0.60	0.75	0.71
	Tied	1.15	0.85	1.03	1.00
$D_0/L = 0, F = 2, L/H = 4$	$\mu = 0.35$	1.42	0.88	1.18	1.04
	Tied	1.59	0.99	1.32	1.17

Let us first evaluate the error induced by using R_{TOT} instead of R in Eq. (7), and therefore erroneously considering the rigid body rotation in the evaluation of the member forces. In the case of a shallow-buried structure with $L/H = 1, D_0/L = 0$ and $F = 1$, the best estimate of the member forces is obtained with the pseudo-triangular pressure (Fig. 19b) and comparison with fem computations results in $M_{inf}/M_{inf}^{fem} = 1.34$ (using R_{TOT}) and $M_{inf}/M_{inf}^{fem} = 1.10$ (using R). A similar comparison can be drawn for a deeply-buried structure with $L/H = 1/2, D_0/L = 1$ and $F = 1$. In this case the best estimate of the member forces is obtained with the pseudo-concentrated forces (Fig. 19a) leading to the following comparison with fem computations: $M_{inf}/M_{inf}^{fem} = 1.24$ (using R_{TOT}) and $M_{inf}/M_{inf}^{fem} = 1.01$ (using R). We can conclude that, in the case of both shallow- and deeply-buried structures, the best estimate of the member forces from the racking ratio is obtained by disregarding rocking, i.e. by using the racking ratio R in Eq. (7).

Table 1 compares the maximum nodal bending moments M_{sup} and M_{inf} in the case of a closed rectangular section (as per Fig. 19), obtained using a simplified approach and pseudo-static FE analysis. These results prompt the following considerations:

- (a) for deeply-buried, 4-sided structures ($D_0/L = 1, L/H = 1$ and $D_0/L = 8, L/H = 2$), evaluating the member moments with a pseudo-concentrated force minimizes the errors; in this case, the overestimations may be as high as 20% (for $L/H = 1, D_0/L = 1$), whereas the results are better for $L/H = 2, D_0/L = 8$;
- (b) for shallow-buried, 4-sided structures ($D_0/L = 0$), the method based on pseudo-triangular pressure leads to better results; for stiff structures with low aspect ratios ($F = 1, L/H = 1$) the error is about 15%, even with rocking, while the maximum error for flexible structures ($F = 3$) with no partialization of

the base foundation is about 30% (for a tied interface) and 11% (for a frictional interface); for large aspect ratios ($L/H = 4$) the underestimations may be as high as 20%.

Likewise, for 3-sided rectangular structures (see Table 2), we can draw the following conclusions:

- (a) for deeply-buried, 3-sided structures ($D_0/L = 1$, $L/H = 1$ and $D_0/L = 8$, $L/H = 2$), the errors are minimized when a pseudo-concentrated force is applied; in this case, the overestimations may be nearly 30% (for $D_0/L = 1$), whereas the results are better for $D_0/L = 8$;
- (b) for shallow-buried, 3-sided structures ($D_0/L = 0$), the method based on a pseudo-concentrated force unexpectedly leads to better results; here again, however, the discrepancy may be as large as 30%.

As a general conclusion, we can say that the errors in the evaluation of the bending moments using simplified analyses based on the pseudo-concentrated force or the pseudo-triangular pressure (Fig. 19) may be as high as 30% by comparison with finite element analyses. The errors are small (about 15%) with base foundation partialization, i.e. for stiff structures with small aspect ratios.

The method based on the pseudo-concentrated force is generally more appropriate for deeply-buried structures, while the pseudo-triangular pressure is more suitable for shallow-buried structures (as Wang suggested), but this may not always be the case. For instance, the pseudo-concentrated force proved more appropriate for shallow-buried, 3-sided rectangular structures.

References

- Anderson, D.G., Geoffrey, R.M., Ignatius, L., Wang, J.N. (2008). Seismic analysis and design of retaining walls, buried structures, slopes and embankments. NCHRP Report 611, Transportation Research Board.
- Basöz N., Mander, J.B., 1999. Enhancement of the Highway Transportation Lifeline Module in HAZUS. Final Prepublication Draft Prepared for The National Institute of Building Sciences, Washington, DC.
- Bobet, A., 2010. Drained and undrained response of deep tunnels subjected to far-field shear loading. *Tunn. Undergr. Space Technol.* 25, 21–31.
- Bobet, A., Fernández, G., Huo, H., Ramirez, J., 2008. A practical iterative procedure to estimate seismic-induced deformations of shallow rectangular structures. *Can. Geotech. J.* 45, 923–938.
- Burnett, D.S., 1987. *Finite Element Analyses from Concepts to Applications*. Addison-Wesley Publishing Company, Reading, Massachusetts.
- CEN, 2004. Eurocode 8: Design of Structures for Earthquake Resistance. Part 1-1: General Rules, Seismic Actions and Rules for Buildings. European Committee for Standardization, Bruxelles, Belgium.
- Das, B.M., 1983. *Fundamentals of soil dynamics*. Elsevier Science Publishing Co., New York.
- Debiasi, E., Gajo, A., Zonta, D., 2012. Seismic vulnerability of shallow buried rectangular structures, Bridge Maintenance, Safety, Management, Resilience and Sustainability, Leiden (NL): CRC Press/Balkema. In: Proc. 6th International Conference on Bridge Maintenance, Safety and Management (IABMAS 2012).
- Hashash, Y.M.A., Hook, J.J., Schmidt, B., Yao, J.I., 2001. Seismic design and analysis of underground structures. *Tunn. Undergr. Space Technol.* 16, 247–293.
- HAZUS-MH MR3, 2003. Multi-hazard Loss Estimation Methodology (Earthquake Model). Technical Manual. Department of Homeland Security Emergency Preparedness and Response Directorate. FEMA. Washington, DC
- Hendron, A.J., Fernández, G., 1983. Dynamic and static design considerations for underground chambers. In: Howard, T.R. (Ed.), *Seismic Design of Embankments and Caverns*. ASCE, New York, pp. 157–197.
- Hibbitt, Karlsson, Sorensen, Inc. 2009. ABAQUS/Standard User's Manual, Version 6.9. Hibbitt, Karlsson & Sorensen, Inc., Pawtucket, RI
- Huo, H., 2005. Seismic Design and Analysis of Rectangular Underground Structures. PhD Thesis, Purdue University, West Lafayette, Indiana.
- Huo, H., Bobet, A., Fernández, G., Ramirez, J., 2005. Load transfer mechanisms between underground structure and surrounding ground: evaluation of the failure of the Daikai Station. *J. Geotech. Geoenviron. Eng., ASCE* 131 (12), 1522–1533.
- Huo, H., Bobet, A., Fernández, G., Ramirez, J., 2006. Analytical solution for deep rectangular underground structures subjected to far-field shear stresses. *Tunn. Undergr. Space Technol.* 21, 613–625.
- Kramer, S.L., 1996. *Geotechnical Earthquake Engineering*. Prentice Hall, New Jersey.
- Lysmer, J., Kuhlemeyer, R.L., 1969. Finite dynamic model for infinite media. *Eng. Mech., ASCE* 95 (4), 859–877.
- Masing, G., 1926. Eigenspannungen und Verfestigung beim Messing. In: *Proceedings, Second International Congress of Applied Mechanics*, pp. 332–335.
- Merritt, J.L., Monsees, J.E., Hendron, A.J., 1985. Seismic design of underground structures. In: Mann, C.D., Kelley, M.N. (Eds.), *Proc. of the 1985 Rapid Excavation Tunnelling Conference*, Society of Mining, Metallurgical and Petroleum Engineers, vol. 1, New York, pp. 104–131.
- Penzien, J., 2000. Seismically induced racking of tunnel linings. *Earthquake Eng. Struct. Dyn.* 29, 683–691.
- Penzien, J., Wu, C.L., 1998. Stresses in linings of bored tunnels. *Earthquake Eng. Struct. Dyn.* 27, 283–300.
- Poulos, H.G., Davis, E.H., 1974. *Elastic Solutions for Soil and Rock Mechanics*. John Wiley & Sons, New York.
- Seed, H.B., Wong, R.T., Idriss, I.M., Tokimatsu, K., 1986. Moduli and damping factors for dynamic analyses of cohesionless soils. *J. Geotech. Eng., ASCE* 112 (11), 1016–1032.
- Zienkiewicz, O.C., Bicanic, N., Shen, F.Q., 1988. Earthquake input definition and the transmitting boundary condition. In: Doltsinis, I.W. (Ed.), *Advances in Computational Nonlinear Mechanics*. Springer-Verlag, pp. 109–138.
- Wang, J.N., 1993. *Seismic Design of Tunnels. A State-of-the-art Approach*. Monograph 7. Parsons Brickerhoff Quade & Douglas, Inc., New York.